論文 / 著書情報
Article / Book Information

Title	Development of Ultrasonic Pulsed Plasma Jet Source for Remote Surface Treatment
Authors	Takashi Ohta, Daisuke Ogasawara, Takahiro Iwai, Hidekazu Miyahara, Akitoshi Okino
Citation	Applied Sciences, Vol. 13, No. 1, 444
Pub. date	2022, 12
Creative Commons	Information is in the article.

applied sciences

MDPI

Article

Development of Ultrasonic Pulsed Plasma Jet Source for Remote Surface Treatment

Takashi Ohta, Daisuke Ogasawara, Takahiro Iwai, Hidekazu Miyahara and Akitoshi Okino *

Laboratory for Future Interdisciplinary Research of Science and Technology, Tokyo Institute of Technology, Yokohama 226-8502, Kanagawa, Japan
* Correspondence: aokino@es.titech.ac.jp; Tel.: +81-45-924-5688

Abstract: We have developed a supersonic pulsed plasma jet device capable of long-distance and high-speed processing, and investigated its basic characteristics for surface treatment applications, mainly in the material and medical fields. The developed apparatus is equipped with a mechanism to transport active species in the plasma to the object to be treated by jetting the generated high-density plasma outward with supersonic pulse jets, which allows the gas flow velocity to increase significantly during pulse jetting compared with plasma generation. This enables the active species in the plasma to reach the treatment target before deactivation, thereby realizing surface treatment at a distance. Measurements using the Schlieren method revealed that the velocity of the jet flow reached Mach 1.7.

Keywords: ultrasonic pulsed plasma; schlieren method; hydrophilic effect

Citation: Ohta, T.; Ogasawara, D.; Iwai, T.; Miyahara, H.; Okino, A. Development of Ultrasonic Pulsed Plasma Jet Source for Remote Surface Treatment. *Appl. Sci.* **2023**, *13*, 444. https://doi.org/10.3390/app13010444

Academic Editor: Bogdan-George Rusu

Received: 19 December 2022
Revised: 23 December 2022
Accepted: 27 December 2022
Published: 29 December 2022

1. Introduction

Atmospheric-pressure plasma has been applied to the decomposition and treatment of industrial waste, trace element analysis, and cutting and processing of high-melting-point materials because it does not require a vacuum vessel or exhaust system and can generate higher-density plasma than low-pressure plasma [1–8]. Recently, however, the development of atmospheric-pressure low-temperature plasma, a type of atmospheric-pressure nonequilibrium plasma, has attracted attention for its application in various industrial and medical fields. This plasma is low-temperature and does not cause thermal damage to the irradiated object; therefore, a wide range of application research is underway, including hydrophilization of surfaces and improvement of adhesive strength in the material field and hemostasis, sterilization, and wound healing in the medical field [9–13]. In a typical atmospheric-pressure low-temperature plasma generator, plasma is generated by supplying plasma-generating gas from a cylinder to a discharge unit and applying a high voltage to the electrodes to cause a discharge. The generated plasma is ejected outward by the gas flow. The active species generated in the plasma are then sprayed onto the material to be treated, causing a variety of useful reactions. However, because the active species in the plasma are deactivated in a short time in the air [14], only objects within a short distance of a few millimeters can be effectively treated, and the treatment efficiency decreases as the distance between the plasma generator and the object to be treated increases [14,15]. If the gas flow rate is increased to allow the active species to reach the target at a distance from the plasma generator, the discharge power density per unit gas volume decreases, causing the plasma density to decrease, which in turn reduces the amount of active species generated, resulting in lower treatment efficiency. Conversely, if the gas flow rate is reduced, it is possible to generate a high-density plasma with a high-power density; however, because the gas flow velocity is reduced, fewer active species reach the target, which also reduces the treatment efficiency [15]. If a sufficient amount of active species can be irradiated onto the target object while maintaining a long distance between the plasma generator and the sample to be treated, it would be useful in actual applications. In this study, a supersonic pulsed plasma jet was developed to realize the high-speed treatment of a sample at a long

distance from an atmospheric-pressure low-temperature plasma generator. In this system, atmospheric-pressure plasma generated between electrodes is pulsed outward with pulsed high-pressure gas, and the active species generated in the plasma are transported to distant objects to be treated. This paper describes the basic characteristics of a supersonic pulsed plasma jet and the results of its surface hydrophilization.

2. Materials and Methods

2.1. Concept and Construction of the Ultrasonic Pulsed Plasma Jet Source

Figure 1 shows a conceptual diagram of the supersonic pulsed plasma jet source. First, high-density plasma was generated by supplying low-speed plasma-producing gas to the discharge. Next, the generated high-density plasma was jetted outward with a supersonic pulse jet to transport the active species in the plasma to the target. The gas flow velocity in the pulse jet is much higher than that in the plasma generation process, allowing the dense active species in the plasma to be irradiated to a distant target before they are deactivated [16]. In the case of short distances, more active species can reach the target; thus, a faster treatment is expected. As the flow velocity increased, the discharge power density per flow rate decreased, resulting in a decrease in treatment effectiveness. In addition, the gas consumption increased; therefore, a short pulse method was used. Figure 2 shows the structure of the supersonic pulsed plasma jet. The housing of the plasma device is made of polyacetal, which is an insulator with two gas channels inside. The discharge section consists of a 2 mm thick machinable ceramic plate, which is an insulator sandwiched between two 2 mm thick copper plate electrodes with a 1 mm hole drilled in the center. Plasma gas was supplied from a cylinder through a gas flow meter and check valve to the enclosure. Pulse jets were generated by briefly opening a 0.5 MPa high-pressure gas with a pulse-controlled solenoid valve (K2-100HA-04-XS0-25, Koganei Corp., New Koganei, Tokyo, Japan). We confirmed that nitrogen, carbon dioxide, air, helium, and argon plasmas were stably generated at a plasma gas flow rate of 3 L/min.

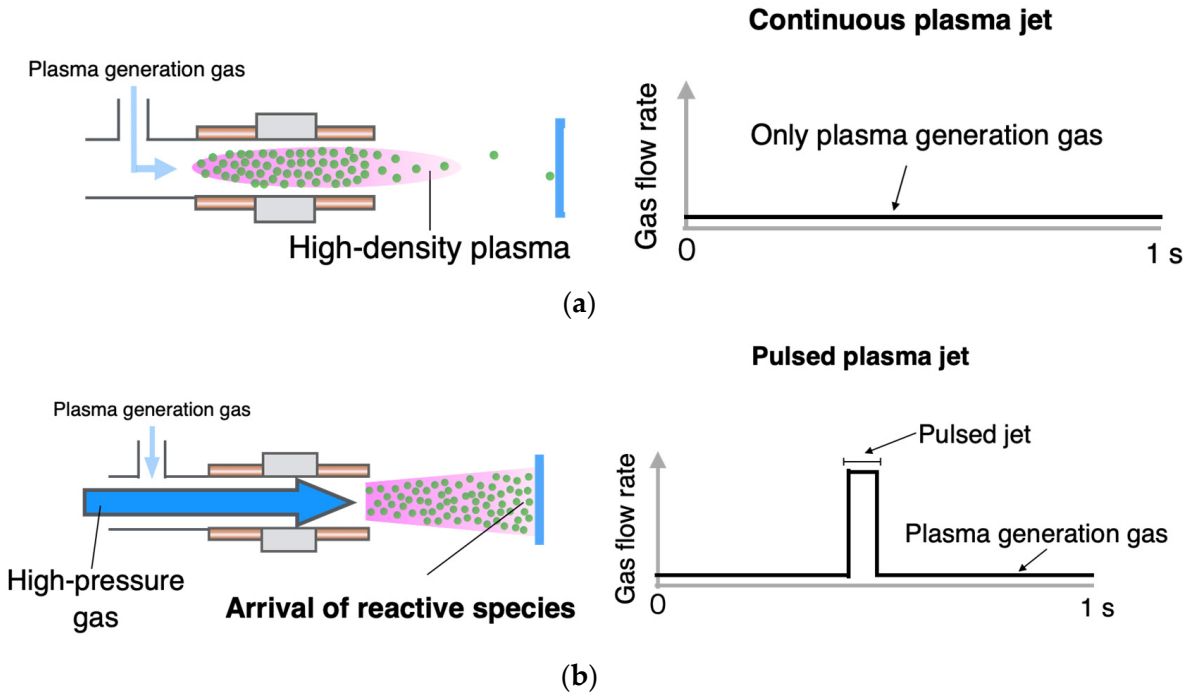

Figure 1. Conceptual diagram of the supersonic pulsed plasma jet: (**a**) continuous plasma jet; (**b**) pulsed plasma jet.

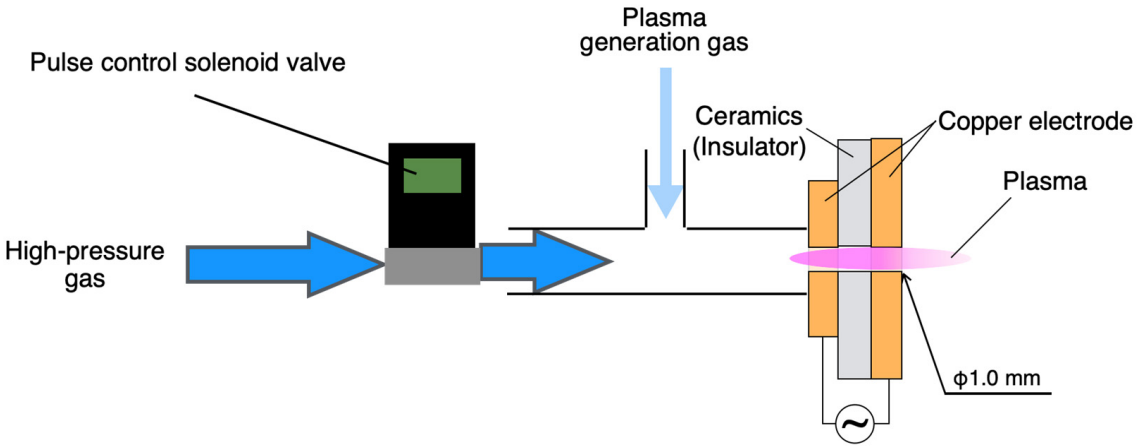

Figure 2. Structure of the supersonic pulsed plasma jet.

2.2. Observation of Ultrasonic Pulsed Plasma Jet

To investigate the extension of the plasma by the pulse jet, a high-speed camera (k5, 8000 fps; Kato Kohken Co., Ltd., Isehara, Kanagawa, Japan) was used to observe the pulsed plasma jet. The plasma jet was generated by opening the solenoid valve of the 0.5 MPa high-pressure gas at a frequency of 1 Hz and a pulse width of 100 ms. The same gas species was used for plasma generation, and high-pressure gases, including nitrogen and helium, were used as the gas species. The schlieren method was used to visualize the plasma gas flow to measure the flow velocity of the supersonic pulsed plasma jet. A high-speed camera (k5, 10,000 fps, Kato Kohken Co., Ltd.) and Schlieren apparatus (SS50 II-L, Kato Kohken Co., Ltd.) were used for the measurements. Plasma gas (3 L/min) was used to generate the plasma, and a solenoid valve was opened at 1 Hz and 100 ms for 0.5 MPa high-pressure gas. The plasma was ejected by opening the solenoid valve of the 0.5 MPa high-pressure gas at 1 Hz for 100 ms.

2.3. Measurement of Electrical Characteristics

The current and voltage characteristics of the prototype device were investigated, and the discharge power was determined. The discharge waveforms were observed using a high-voltage probe (HVP39pro, Pintek Electronics Co., New Taipei, Taiwan), current probe (TCP303, TCPA300, Tektronix Co., Beaverton, OR, USA), and oscilloscope (TDS-680B, Tektronix Co., USA). Plasma was generated using 3 L/min plasma gas, and then the solenoid valve of the 0.5 Mpa high-pressure gas was opened at 1 Hz for 100 ms to eject the plasma. The same gas species were used as the plasma generator gas and high-pressure gas: nitrogen, carbon dioxide, air, argon, and helium.

2.4. Dependence of Hydrophilic Effect on Plasma Gas Species

The hydrophilic effect of plasma has been reported to depend on the gas species [17]. In addition, gas species may be limited by gas price and safety considerations. The hydrophilic effect of plasma on each gas species was evaluated using supersonic pulsed plasma jets.

The contact angle was determined by measuring the contact angle of a water droplet resting on a copper plate (C1100P) surface and the evaluation was based on the magnitude of the angle. The smaller the contact angle of a solid surface, the more hydrophilic the surface, and the easier it is for water and other solvents to wet it, whereas the larger the contact angle, the less hydrophilic the surface, and the easier it repels water.

The contact angle measurement method is defined by JIS as the JIS R 3257 Wettability test method for glass substrate surfaces [18]. The principle of the contact angle measurement method is illustrated in the figure. A drop of water was then placed on the horizontal specimen. If the volume of the droplet is 4 μL or less, the shape of the droplet can be

regarded as a part of a sphere, and the following relationship is established between the contact angle θ and droplet shape.

$$\theta = 2\tan^{-1}\frac{h}{r} \quad (1)$$

where r is the radius of the water droplet on the surface in contact with the specimen (mm) and h is the height from the specimen surface to the apex of the droplet (mm). The values of r and h were measured, and the contact angles were obtained using the relational equation.

In the experiment, a contact angle meter (PG-X, Matsubo Co., Ltd., Minato-ku, Tokyo, Japan) was used to measure the contact angle between the specimen surface and water droplets to evaluate the hydrophilic effect. The volume of each water droplet was 2 μL.

The plasma treatment time was 1 s, the plasma irradiation distance was 5–40 mm, and the supersonic plasma was irradiated at 13 Hz and 10 ms. The gas species used for the supersonic plasma were nitrogen, carbon dioxide, air, argon, and helium.

3. Results and Discussion

3.1. Observation of Plasma Stretching by Ultrasonic Pulsed Plasma

Figure 3 shows the observation of the nitrogen plasma. When plasma was generated, the emission was weak, and the stretching distance of the nitrogen plasma was approximately 3 mm; however, when the nitrogen plasma was pulsed jetted, strong emission was observed, and the stretching distance increased to approximately 6 mm. The extension distance of the plasma was approximately twice that of the plasma generated by the pulsed jet. Figure 3 shows the observation results for the helium plasma. During plasma generation, the helium plasma could not be captured by the camera because of weak luminescence; however, the luminescence became stronger when the helium plasma was ejected by the pulse jet, and the extension distance of the helium plasma increased to approximately 7 mm. In addition, a luminescence that appeared as a shock diamond-shaped shock waves, called shock diamonds, was observed in the plasma. These results indicate that the plasma can be jetted far away by the pulsed jet and that the plasma jet velocity may reach supersonic speeds.

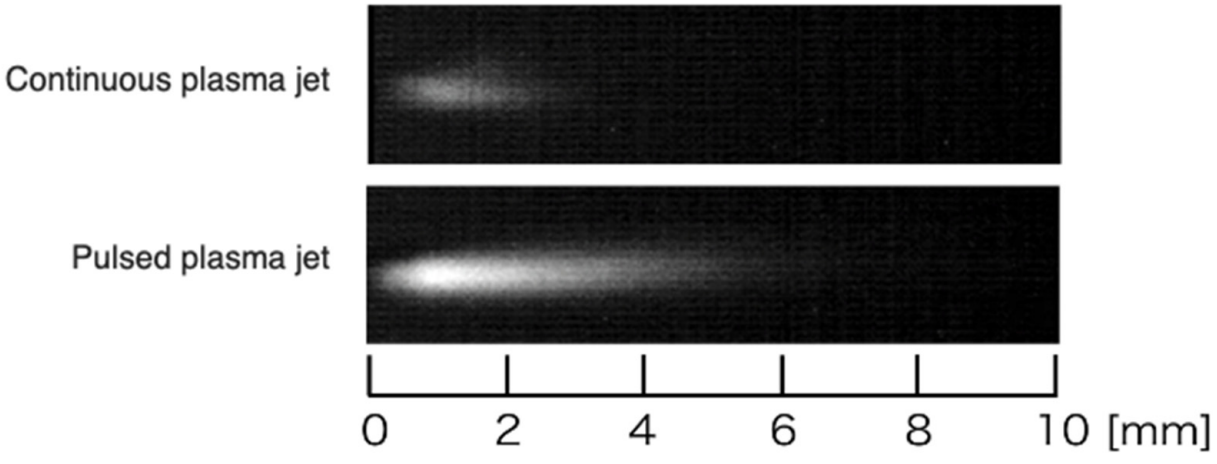

(**a**)

Figure 3. *Cont.*

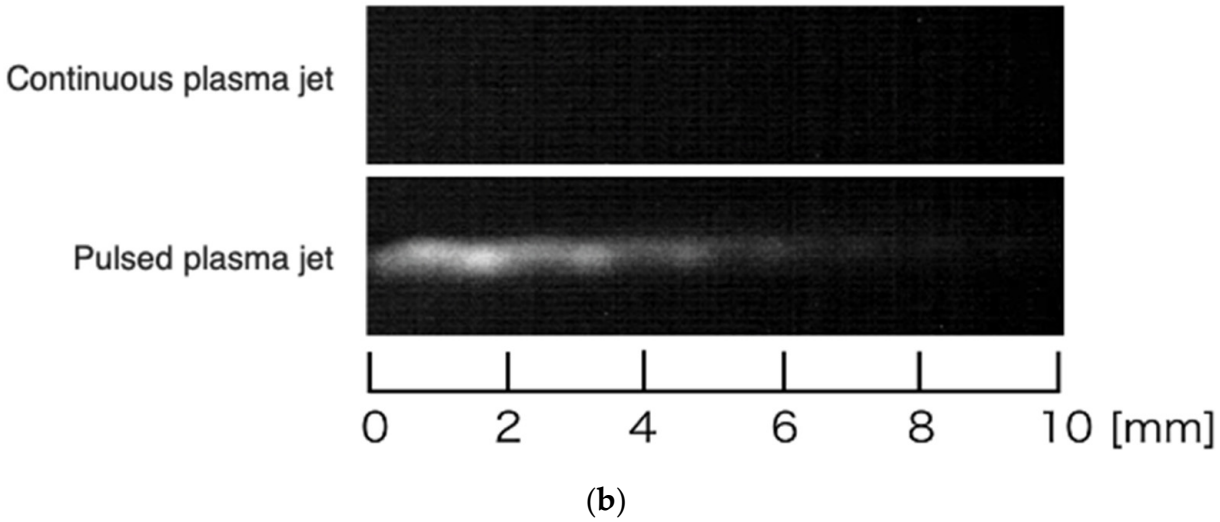

Figure 3. Photographs of plasma: (**a**) nitrogen plasma; (**b**) helium plasma.

3.2. Measurement of Plasma Gas Flow Rate by the Schlieren Technique

The schlieren method is a technique for visualizing the flow of transparent media, such as air or water, and the visualized image can reveal the flow state and velocity. Therefore, it is widely used as a method for analyzing the flow of plasma jets [19,20]. In a typical configuration of the schlieren method, light from a light source is collimated by a convex lens or concave mirror, and the object is placed in the collimated light. The object was placed under collimated light. The light was then focused again by a convex lens, and a knife edge was placed such that it slightly covered the focal point from one side. When the density of the fluid changes with the subject, the refractive index of light changes. The path of the collimated light rays passing near the subject was bent, causing the focal point to change when the light was focused. This change intercepts light that is deflected to the knife-edge side, resulting in a brightness difference in the image captured by the camera ahead, enabling the visualization of the density field of the fluid [21]. The larger the density gradient, the more clearly the schlieren method can visualize the density field; therefore, it is often applied to scenarios such as high-speed flows and combustion but rarely to low-speed flows. However, because plasma causes a density change in the fluid owing to heating by the discharge, visualization is possible even when the flow velocity of the plasma jet is relatively slow [22]. The sound waves generated at an arbitrary point in the gas in the plasma jet then spread from that position to the surroundings at the speed of sound a. If the gas through which the sound wave travels is stationary relative to source P, the sound wave travels spherically to infinity at a given time. If the gas moves at velocity v relative to the source, the sound wave travels at the speed of sound relative to the flow. Therefore, the sound wave propagates at a speed of $a + \mathrm{v}$ in the direction of the flow and $a - \mathrm{v}$ in the direction opposite to the flow. When velocity v of the gas exceeds the speed of sound a and becomes supersonic, multiple sound waves overlap, generating a shock wave [23]. Shock waves are formed in the same manner when the gas is jetted out of a nozzle at supersonic speeds. However, the shockwave varies depending on the expansion state of the gas. For example, if the nozzle outlet pressure Pe is greater than the atmospheric pressure Pa (Pe > Pa), an underexpanded jet is formed. When Pe = Pa, an appropriate expansion jet was produced. If Pe < Pa, the jet is overexpanded. In the case of an appropriately expanded jet and an underexpanded jet, the following relationship holds for the Mach number of the flow M_1 and shock wave angle β [24].

$$\sin\beta = \frac{a}{v} = \frac{1}{\mathrm{M}_1} \tag{2}$$

where v is the gas velocity, $a = \left(\sqrt{\kappa RT/M}\right)$ is the sound velocity, and is a function of specific heat ratio κ, R, T, and M. In the case of an overexpanded jet, the flow narrows at a turning angle θ to approach an oblique shockwave. The following relationship is then established among Mach number M_1, shock wave angle β, turning angle θ, and specific heat ratio κ [25]:

$$\tan\theta = \frac{2\cot\beta\left(M_1^2 sin^2\beta - 1\right)}{M_1^2(\kappa + \cos 2\beta) + 2} \quad (3)$$

Using these relations, the Mach number can be calculated from the value of the shock wave angle β obtained from the schlieren image. The gas velocity can also be calculated from the product of the Mach number and the sound velocity of the gas.

3.3. Extension of Ultrasonic Pulsed Plasma Jet

Figure 4 shows a schlieren image of a supersonic pulsed plasma jet for each gas species, and Table 1 shows the maximum values of the Mach number and gas velocity. In the schlieren image, the left side is the plasma jet side, and the right side is the atmospheric side. In the nitrogen, carbon dioxide, air, and argon plasmas, shock waves were generated 2 ms after the solenoid valve was opened, and diamond-shaped shock waves were observed after 3 ms. The bright and dark areas in the shock diamonds caused by the compressional and expansive waves suggest that the flow of the pulsed plasma jet is an underexpanded jet. The shock diamonds extended toward the atmosphere with a narrowing of the shock wave angle every 1 ms, reaching their maximum extension distance after 6 ms in argon plasma and after 7 ms in nitrogen, carbon dioxide, and air plasma. The maximum Mach number was calculated to be Mach 1.6 for argon plasma and Mach 1.7, for nitrogen, carbon dioxide, and air plasmas, with gas velocities of 501, 585, 452, and 575 m/s, respectively. In contrast, the helium plasma was confirmed to have a Mach number of 1 (1014 m/s) or higher by observing a shock wave near the plasma jet; however, it was difficult to calculate the detailed gas flow velocity because the schlieren image was unclear compared with the plasma of other gas species.

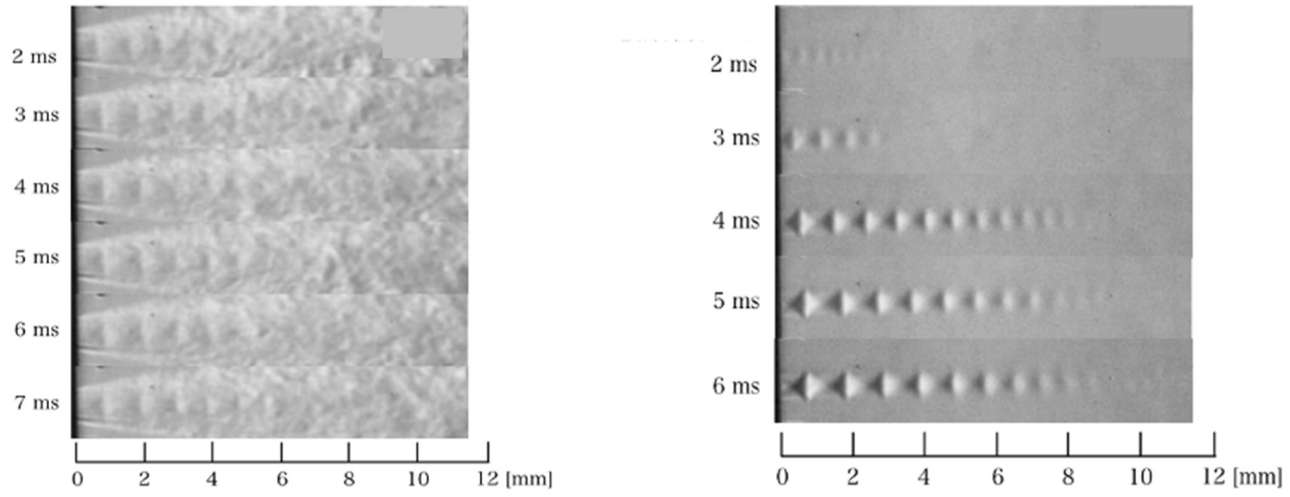

Figure 4. *Cont.*

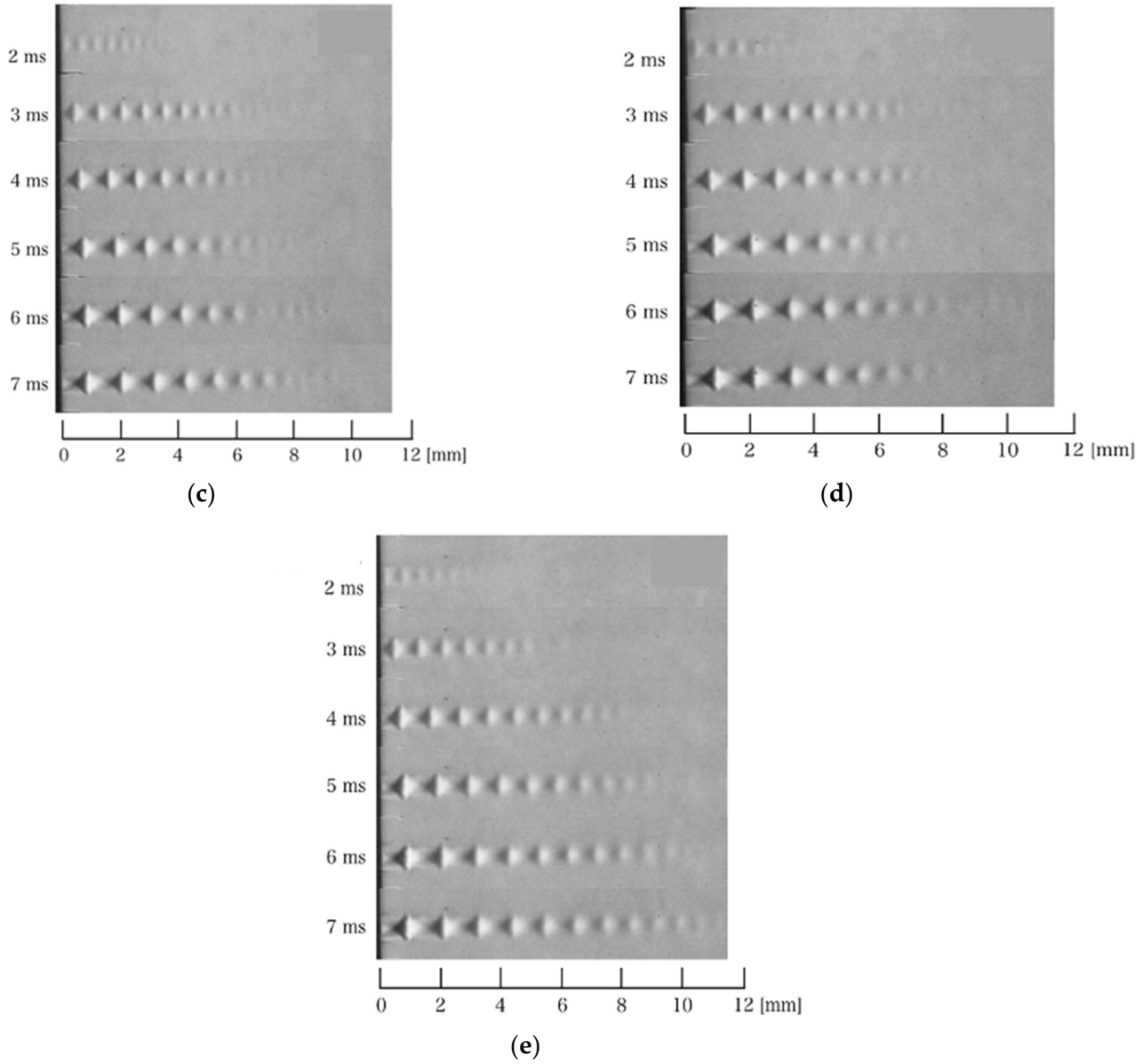

Figure 4. Schlieren image of pulsed plasma jet: (**a**) helium plasma; (**b**) argon plasma; (**c**) nitrogen plasma; (**d**) air plasma; (**e**) carbon dioxide plasma.

Table 1. Mach number of plasma and gas flow velocities for each gas type.

Plasma Gas Type	Mach Number	Sound Velocity [m/s] (25 °C)	Gas Velocity [m/s]
Ar	1.6	322	501
N_2	1.7	352	585
CO_2	1.7	271	452
Air	1.7	347	575
He	>1	1014	>1014

On the basis of Mach number measurements, the gas flow velocities of pulsed plasma jets of each gas species were compared with those of a conventional plasma system without pulsed operation, that is, a conventional plasma system. The gas flow velocity of the conventional system was 64 m/s, calculated from the gas flow rate (3 L/min) and plasma jet outlet

area (0.79 mm^2). Therefore, the pulsed plasma jets of each gas type evidently emit plasma with a velocity approximately 7–16 times higher than that of the conventional system.

3.4. Evaluation of Hydrophilic Effect Dependence on Plasma Gas Type

Figure 5 shows the results of hydrophilic treatment with plasma for each gas type. The horizontal axis represents the irradiation distance, and the vertical axis represents the contact angle. The contact angle was measured at five points and the average value was obtained. This procedure was repeated three times, and the mean value and standard deviation were further obtained. When nitrogen and carbon dioxide supersonic plasmas were irradiated at a distance of 5 mm, the contact angles were 33° and 53°, respectively, and the maximum contact angle was 14° lower than that of the conventional system. For helium and argon supersonic plasmas, the contact angles were lower than those of the conventional system when the irradiation distance was ≥10 mm. In particular, in helium supersonic plasma, the contact angle decreased by a maximum of 20° when the irradiation distance was 10 mm, and the irradiation distance at which the hydrophilic effect appeared increased from approximately 20 to 40 mm. The sound velocity of helium is 1014 m/s, which is more than three times higher than those of nitrogen (352 m/s) and carbon dioxide (271 m/s). Therefore, compared with supersonic plasmas of other gases, the active species are ejected farther in a shorter time, which is thought to improve the hydrophilicity of the plasma. In contrast, when helium and argon plasma were irradiated at a distance of 5 mm, the contact angles were 58° and 55°, respectively, in the conventional system, but increased to 61° and 68° in the supersonic plasma. This is because the plasma and atmospheric components did not react sufficiently, and the active species of oxygen and nitrogen that contribute to hydrophilicity were not generated. These results confirm the improved hydrophilicity of nitrogen, carbon dioxide, argon, and helium supersonic plasmas. Evidently, nitrogen supersonic plasma is effective in improving hydrophilicity for short-distance treatment, whereas helium supersonic plasma is effective for long-distance treatment.

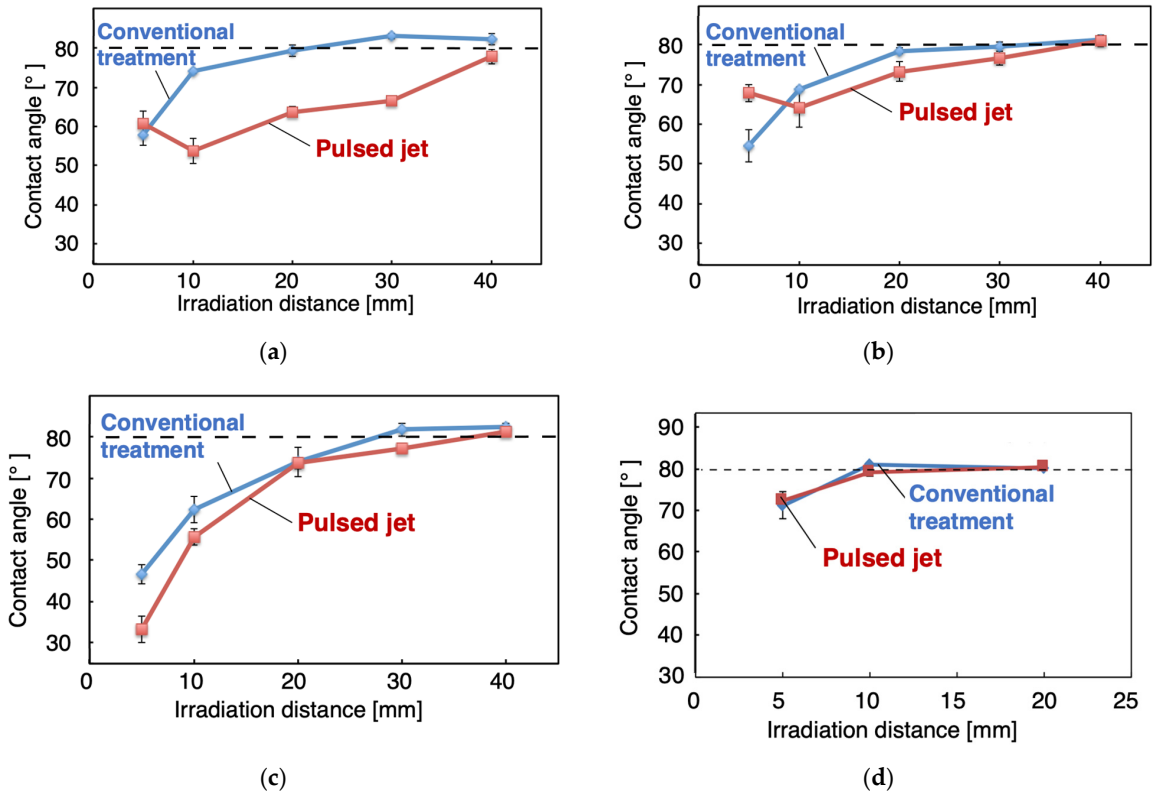

Figure 5. *Cont.*

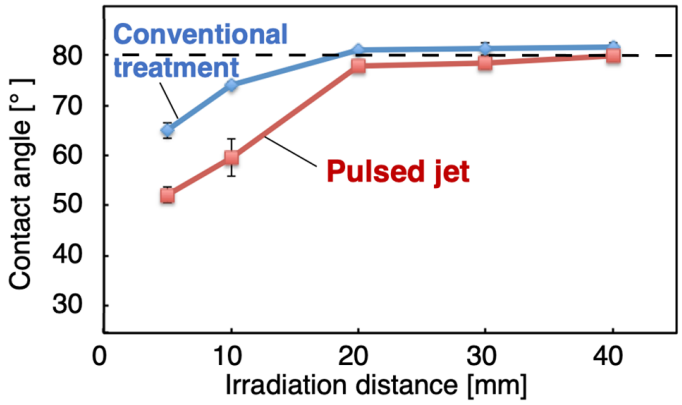

(**e**)

Figure 5. Relationship between irradiation distance and hydrophilic effect: (**a**) helium plasma; (**b**) argon plasma; (**c**) nitrogen plasma; (**d**) air plasma; (**e**) carbon dioxide plasma.

4. Conclusions

This study describes the development of a supersonic pulsed plasma jet device capable of long-distance and high-speed processing and investigates the basic characteristics of the device for surface treatment applications, mainly in the material and medical fields. The developed device was equipped with a mechanism to transport the active species in the plasma to the object to be treated by jetting the generated high-density plasma outward with a supersonic pulse jet. The high-density active species in the plasma can be irradiated to distant targets before they are deactivated. In the case of short distances, more active species can reach the target; thus, faster processing can be expected. If the constant flow velocity is increased, the discharge power density per flow rate decreases, and the treatment effect decreases. In addition, gas consumption increases; therefore, a short-pulse method was used. Observation of the plasma by a high-speed camera confirmed that the plasma emission intensity increased, and the extension distance increased when the plasma was discharged by a pulsed jet. The velocity of the supersonic pulsed plasma jet was measured using the schlieren method, and it was found that the pulsed plasma jet was a short knife jet. The maximum Mach number was calculated to be Mach 1 or higher for helium plasma, Mach 1.6 for argon plasma, and Mach 1.7 for nitrogen, carbon dioxide, and air plasma. Power measurements confirmed that the helium and argon plasmas during the pulsed jet increased in power, whereas the carbon dioxide plasma decreased in power. The difference in the power is considered to depend on the breakdown voltage. The above results suggest that the reachable distance of the active species is extended, and the efficiency of surface treatment by plasma is improved. The effect of the plasma gas type on the hydrophilic effect was investigated. The maximum hydrophilic effect was observed when the nitrogen supersonic plasma was irradiated at 13 Hz for 10 ms, and the contact angle was reduced by a maximum of 14°. Additionally, it was found that nitrogen supersonic plasma was effective in improving hydrophilicity for short-distance treatment and helium supersonic plasma for long-distance treatment.

Author Contributions: Conceptualization, T.O.; investigation, T.O. and D.O. and T.I. and H.M.; project administration, A.O. All authors have read and agreed to the published version of the manuscript.

Funding: This research received no external funding.

Institutional Review Board Statement: Not applicable.

Informed Consent Statement: Not applicable.

Data Availability Statement: Data available in a publicly accessible repository.

Acknowledgments: We thank Koichi Fujimura of Kato Koken Co., Ltd., who helped us with the schlieren measurements and analysis.

Conflicts of Interest: The authors declare no conflict of interest associated with this manuscript.

References

1. Takemura, Y.; Kubota, Y.; Yamaguchi, N.; Hara, T. Development of atmospheric plasma jet with long flame. *IEEE Trans. Plasma Sci.* **2009**, *37*, 1604–1606. [CrossRef]
2. Yanagawa, Y.; Kawano, H.; Kobayashi, T.; Miyahara, H.; Okino, A.; Mitsuhara, I. Direct protein introduction into plant cells using a multi-gas plasma jet. *PLoS ONE* **2017**, *12*, e0171942. [CrossRef] [PubMed]
3. Kurosawa, M.; Takamatsu, T.; Kawano, H.; Hayashi, Y.; Miyahara, H.; Ota, S.; Okino, A.; Yoshida, M. Endoscopic Hemostasis in Porcine Gastrointestinal Tract Using CO_2 Low-Temperature Plasma Jet. *J. Surg. Res.* **2019**, *234*, 334–342. [CrossRef] [PubMed]
4. Nomura, Y.; Takamatsu, T.; Kawano, H.; Miyahara, H.; Okino, A.; Yoshida, M.; Azuma, T. Investigation of blood coagulation effect of nonthermal multigas plasma jet in vitro and in vivo. *J. Surg. Res.* **2017**, *219*, 302–309. [CrossRef] [PubMed]
5. Shigeta, K.; Koellensperger, G.; Rampler, E.; Traub, H.; Rottmann, L.; Panne, U.; Okino, A.; Jakubowski, N. Sample introduction of single selenized yeast cells (*Saccharomyces cerevisiae*) by micro droplet generation into an ICP-sector field mass spectrometer for label-free detection of trace elements. *J. Anal. At. Spectrom.* **2013**, *28*, 637. [CrossRef]
6. Shigeta, K.; Traub, H.; Panne, U.; Okino, A.; Rottmann, L.; Jakubowski, N. Application of a micro-droplet generator for an ICP-sector field mass spectrometer—Optimization and analytical characterization. *J. Anal. At. Spectrom.* **2013**, *28*, 646. [CrossRef]
7. Iwai, T.; Takahashi, Y.; Miyahara, H.; Okino, A. Development of the atmospheric plasma soft-ablation method (APSA) for elemental analysis of materials on heat-sensitive substrates. *Anal. Sci.* **2013**, *29*, 1141–1145. [CrossRef]
8. Miyahara, H.; Iwai, T.; Nagata, Y.; Takahashi, Y.; Fujita, O.; Toyoura, Y.; Okino, A. Development and fundamental investigation of He plasma ionization detector (HPID) for gas chromatography using DC glow discharge. *J. Anal. At. Spectrom.* **2014**, *29*, 105–110. [CrossRef]
9. Graves, D.B. The emerging role of reactive oxygen and nitrogen species in redox biology and some implications for plasma applications to medicine and biology. *J. Phys. D Appl. Phys.* **2012**, *45*, 263001. [CrossRef]
10. Kalghatgi, S.U.; Fridman, G.; Cooper, M.; Nagaraj, G.; Peddinghaus, M.; Balasubramanian, M.; Vasilets, V.N.; Gutsol, A.F.; Fridman, A.; Friedman, G. Mechanism of Blood Coagulation by Nonthermal Atmospheric Pressure Dielectric Barrier Discharge Plasma. *IEEE Trans. Plasma Sci.* **2007**, *35*, 1559–1566. [CrossRef]
11. Fridman, G.; Peddinghaus, M.; Balasubramanian, M.; Ayan, H.; Fridman, A.; Gutsol, A.; Brooks, A. Blood Coagulation and Living Tissue Sterilization by Floating-Electrode Dielectric Barrier Discharge in Air. *Plasma Chem. Plasma Process.* **2006**, *26*, 425–442. [CrossRef]
12. Iseki, S.; Nakamura, K.; Hayashi, M.; Tanaka, H.; Kondo, H.; Kajiyama, H.; Kano, H.; Kikkawa, F.; Hori, M. Selective killing of ovarian cancer cells through induction of apoptosis by nonequilibrium atmospheric pressure plasma. *Appl. Phys. Lett.* **2012**, *100*, 113702. [CrossRef]
13. Vandamme, M.; Robert, E.; Lerondel, S.; Sarron, V.; Ries, D.; Dozias, S.; Sobilo, J.; Gosset, D.; Kieda, C.; Legrain, B.; et al. ROS implication in a new antitumor strategy based on non-thermal plasma. *Int. J. Cancer.* **2012**, *130*, 2185–2194. [CrossRef]
14. Mizuno, A. Sterilization by oxygen radicals. *J. Appl. Phys.* **2003**, *72*, 457–461.
15. Yanagisawa, Y.; Yoshioka, Y. Remote surface modification of plastics by atmospheric pressure barrier discharge. *IEEJ Trans. A.* **2007**, *127*, 303–308.
16. Hasan, M.I.; Walsh, J.L. Influence of gas flow velocity on the transport of chemical species in an atmospheric pressure air plasma discharge. *Appl. Phys. Lett.* **2017**, *110*, 134102. [CrossRef]
17. Miyahara, S.; Shibata, M.; Oshita, T.; Takamatsu, T.; Takamatsu, T.; Okino, A. Hydrophilic treatment of polyimide film by damage-free multi-gas plasma jet. *Chem. Eng. J.* **2013**, *39*, 372–377.
18. Japanese Standards Association. *JIS Handbook 33 Glass*; Japanese Standards Association: Tokyo, Japan, 2007.
19. Bradley, J.W.; Oh, J.; Olabanji, O.T.; Hale, C.; Mariani, R.; Kontis, K. Schlieren photography of the outflow from a plasma jet. *IEEE Trans. Plasma Sci.* **2011**, *39*, 2312–2313. [CrossRef]
20. Boselli, M.; Colombo, V.; Gherardi, M.; Laurita, R.; Liguori, A.; Sanibondi, P.; Simoncelli, E.; Stancampiano, A. Characterization of a cold atmospheric pressure plasma jet device driven by nanosecond voltage pulses. *IEEE Trans. Plasma Sci.* **2015**, *43*, 713–725. [CrossRef]
21. Matsuno, T.; Honami, S.; Fujii, K.; Sekimoto, S.; Iida, A. Fluid measurement methods. *J. Plasma Fusion Res.* **2015**, *91*, 661–664.
22. Matsuno, T.; Maeda, K.; Fujita, N.; Haruna, K.; Yamada, G.; Kawazoe, H. On the mechanism of bluff body flow control by pulsed plasma actuator. *J. Fluid Sci. Technol.* **2014**, *9*, JFST0048. [CrossRef]
23. Katoh Koken Corporation, Home Page. 2016. Available online: http://www.kk-co.jp/visible/schlieren.php (accessed on 20 November 2022).
24. Ikui, T.; Matsuo, K. *Mechanics of Compressible Fluids*; Rikogaku-Sha: Tokyo, Japan, 1985.
25. Sakaki, K.; Shimizu, Y.; Goda, Y. Effect of expansion state of combustion gas jet on high speed flame spray process. *J. Jpn. Inst. Met.* **1999**, *63*, 269–276. [CrossRef] [PubMed]